Computerized Three-dimensional Cephalometric Template for Thai Adults

Jeenarat Duangsuwan
Mahidol University
Somchart Raocharernporn
Mahidol University
Sasipa Thiradilok
Mahidol University
Somchai Manopatanakul
msomchai@rocketmail.com

Mahidol University

Research Article

Keywords: Template, Three-dimensional, 3D, Cephalometric analysis, CBCT, Orthodontics

Posted Date: March 15th, 2022

DOI: https://doi.org/10.21203/rs.3.rs-1435588/v1

Additional Declarations: No competing interests reported.

Version of Record: A version of this preprint was published at Heliyon on April 1st, 2023. See the published version at https://doi.org/10.1016/j.heliyon.2023.e15077.

Abstract

Background: With its increased accessibility, the use of cone-beam computed tomography (CBCT) is gradually expanding around the world. CBCT images can be reconstructed to form three-dimensional (3D) images that resemble the actual morphology of a patient's skull, and this can be useful in cephalometric analysis and teledentistry. In this study, we aimed to develop 3D templates for Thai adults based on cephalometric landmark coordinates obtained from skull CBCT scans.

Methods: Full head CBCT scans of a total of 39 subjects (18 males and 21 females) were obtained. The scans were taken in a normal head position and the coordinates of 21 important cephalometric landmarks were identified using Slicer 4.10.2 software. Intraclass correlation coefficients (ICC) and Bland-Altman plots were used to assess inter- and intra-examiner reliability. Independent samples *t*-tests were used to compare all mean coordinates between male and female subjects.

Results: All landmark coordinates were accurately traced and analyzed. ICC values of 0.97-0.99 were obtained, confirming measurement reliability. Most of the Z-axis coordinates were statistically different between males and females. As a result, using the means of the landmark coordinates, 3D cephalometric templates for adult Thai males and females were generated separately.

Conclusion: 3D cephalometric templates for Thai adults were created, and it is recommended to be used most effectively for Thai adults to detect deviations in skull morphology from the population norm.

Background

The accessibility of cone-beam computed tomography (CBCT) has increased substantially in dentistry, particularly in the field of orthodontics[1–5]. This highlights the importance of developing a three-dimensional (3D) cephalometric norm, in particular for use in orthognathic surgery. While automated tracing of anatomical landmarks is still in its infancy[6, 7], 3D cephalometric templates may eventually provide a user-friendly tool for rapid diagnosis. These templates could be superimposed onto skull CBCT images to outline the major skeletal discrepancies. This will act as virtual media for teledentistry in diagnosing, monitoring, and planning the correction of the craniofacial structures.

Before the advancements in 3D imaging, two-dimensional (2D) cephalometric radiographs were the main means of skeletal assessment, but the limitations of this technique are evident[8]. The main disadvantage of a 2D image is that only 2D data can be generated from a subject which is 3D in real life[9]. As a result, the images in these 2D radiographs are prone to have projection and magnification errors. Besides that, these 2D radiographs require manual landmark identification and tracing, which can be tedious and time-consuming. In order to reduce the factor of human error, these tracings would need to be reassessed by experienced orthodontists. An accumulation of these inaccuracies would inevitably lead to measurement errors which may affect subsequent diagnosis and treatment planning. Because of these reasons, cephalometric templates for these 2D images have been previously developed and shown to reduce time

consumption and the margin of error[10–14]. With this idea in mind, having a 3D cephalometric template coupled with the advantage of having more complete data from the 3D image would potentially produce a more effective workflow in anatomical landmark tracing for a more precise diagnosis.

Currently, artificial intelligence (AI) is one of the most compelling areas of interest for healthcare professions, and orthodontists who are faced with large amounts of complex data while making decisions are not exempted. Machine learning (ML), a subset of artificial intelligence (AI), is extremely efficient in this era of high-tech development. With the help of ML, cephalometric templates may be used to replace the often complicated sets of values derived from laborious line and angular measurements, especially for decision-making in orthognathic surgery.

In addition, many studies have demonstrated that craniofacial measurements vary between ethnic groups, age, and gender. These variables may greatly affect the accuracy of template constructions. Therefore, with the increased use of CBCT, there is an urgent need to derive a 3D cephalometric norm for the Thai population. As such, the purpose of this study was to generate 3D cephalometric templates from a group of Thai adults with normal occlusion. Age, gender, and racial group were among the factors that must be carefully considered in developing this template.

Methods

Sample characteristics

This study was approved by the Institutional Review Board of the Faculty of Dentistry/Faculty of Pharmacy, Mahidol University (COE. No. MU-DT/PY-IRB 2020/084.2412). CBCT images of the skull of Thai adults with normal occlusion were obtained. The study sample consisted of 39 subjects (18 males and 21 females) that were included based on the following criteria:

- Thai adults between the ages of 18 to 40 years
- Angle's Class I occlusions
- The presence of an entirely permanent dentition (not including the permanent third molars)
- No obvious facial asymmetry or dysmorphology
- No history of orthodontic treatment or head and neck surgery
- An overjet of 1–4 mm. and overbite of 25–50%

Data capture and processing

All subjects underwent CBCT imaging using a voxel size of 0.40 mm, voltage of 90 kVp, and a current of 8.0 mA using a Planmeca ProFace (Planmeca USA, Inc.; Roselle, IL, USA). The subjects wore a lead apron during the procedure and were instructed to maintain a natural head position and centric occlusion. All CBCT images were saved as .dcm (Digital Imaging and Communications in Medicine, DICOM) files for further processing.

Localization of skull anatomical landmarks

3D Slicer software (version 4.10.2)[15] was used to import the DICOM files of the CBCT images and standardize them in three coordinate planes. The sagittal plane (ZY) was set as the plane allowing the closest mirrored symmetry of the facial structures. The transverse plane (XZ) was accepted to be parallel to the ANS-PNS line. Then, using 'Segment Editor' modules, structures of the bone and teeth were selected to generate a volumetric image with a threshold range of 500 to 3095.

When viewing coronal slice of the CBCT image, the x-axis was directed from left to right, the y-axis from back to front, and the z-axis from top to bottom. The sagittal slice of the scan was aligned to the natural position of the head, followed by aligning the coronal slice such that a line connecting the zygomaticofrontal sutures bilaterally was approximately parallel to the true horizontal plane. The axial slice was then adjusted to align the mid-palatal suture approximately perpendicular to the true horizontal reference plane.

21 cephalometric landmarks employed in this study are defined in Table 1. All landmarks were identified by a practitioner who had been trained and calibrated by an orthodontic specialist to locate the 3D landmarks using a set of ten CBCT images. The measurements were repeated after a one-week interval in order to assess intra-examiner reliability. Spherical markers of 1 mm diameter were placed to indicate the location of each landmark, and the software produced the coordinates from the center of these spherical markers. The x, y, and z coordinates of each landmark were defined based on the Cartesian system used by Zamora et al[16] (See Table 1).

To standardize and to aid in the selection of the most precise anatomic landmark identification across three spatial planes, the software allowed for simultaneous viewing of the same spatial location in all three sagittal, coronal, and axial planes, each in a separate window. A fourth window enabled the anatomical point to be viewed on a volume-rendered window displaying a 3D image of the skull (Fig. 1). For each sample, the investigator selected a landmark in the first visible slice, then moved mesiodistally, superior-inferiorly, and antero-posteriorly to refine its position. To improve the visualization of the landmarks, the zoom and contrast settings in the software were attuned. The coordinate system obtained from the software was in the Right-Anterior-Superior (RAS) format.

The practitioner identified 21 landmarks in 39 CBCT images at two separate time intervals, where each point yielded three coordinate values (R, A, and S), resulting in a total of 234 values for each point and 4,914 values for all 21 points.

Table 1

Definition of the three spatial planes of 21 cephalometric landmarks used in this study[6]

Name	Anatomical definition	Sagittal or Lateral view	Coronal or Frontal view	Axial view
Sella turcica (S)	Anteroposterior midpoint of the pituitary fossa of the sphenoid bone	Midpoint of the anteroposterior width	Midpoint of the lateral width of the fossa, determined anteroposteriorly by the other two slices	Midpoint of the anteroposterior and lateral width of the fossa
Nasion (N)	Most anterior point of the frontonasal suture.	Most anterior point	Midpoint	Most anterior and midpoint of the anterior contour
Point A (A)	Most posterior point of the maxillary curvature, between the anterior nasal spine and the supradental point	Most posterior point	Midpoint determined anteroposteriorly by the other two slices cortex	Most anterior and midpoint
Point B (B)	Most posterior point of the anterior surface of the mandibular symphysis	Most posterior point	Midpoint determined anteroposteriorly by the other two slices	Most anterior and midpoint.
Anterior nasal spine (ANS)	Most anterior point of the maxillary process in the nasal floor region	Most anterior point	Most anterior and midpoint	Most anterior and midpoint
Posterior nasal spine (PNS)	Most posterior and midpoint of the palatine bone contour	Most posterior point	Most posterior and midpoint	Most posterior and midpoint
Right and Left orbital (RtOr/LtOr)	Most anterosuperior point of the infraorbital margin of the right and left orbital	Most anterior point	Uppermost and midpoint	Most anterior point
Right and Left Porion (RtPo/LtPo)	Uppermost and midpoint of the external right roof of the auditory meatus	Uppermost and midpoint	Uppermost point	Midpoint, determined superoinferiorly by the other two slices
Incisal edge of upper right and left central incisor (RtUI/LtUI)	Lowest point of the incisal edge of the upper right and left central incisor	Lowest point	Midpoint of the mesiodistal width	Most anterior and midpoint of the mesiodistal width

Name	Anatomical definition	Sagittal or Lateral view	Coronal or Frontal view	Axial view
Apical root of upper right and left central incisor (RtUA/LtUA)	Highest point on the apical root of the upper right and left central incisor	Highest point	Upper most of the mesiodistal width	Most central point
Incisal edge of lower right and left central incisor (RtLI/LtLI)	Most superior point of the incisal edge of the lower right and left central incisor	Highest point	Midpoint of the mesiodistal width	Most anterior and midpoint of the mesiodistal width
Apical root of lower right and left central incisor (RtLA/LtLA)	Lowest point of the root of the lower right and left central incisor	Lowest point	Lowest point of the mesiodistal width	Most central point
Gnathion (Gn)	Most anteroinferior point of the mandibular symphysis	Most anterior and lowest point	Mid- and lowest point	Most anterior, lowest and midpoint
Right and left Gonion (RtGo/LtGo)	Most posterior point of the posterior edge of the right and left branch. Bisection of the tangents of the posterior edge of the branch and the lower body	Most posterior point	Most posterior and midpoint	Most posterior point, determined superoinferiorly by the other two slices

Table 2
Intra-examiner reliability values of R, A, and S coordinates for all landmarks.

	R			A			S		
Landmarks	ICC (95% CI)	Bias ± S.D.	LOA	ICC (95% CI)	Bias ± S.D.	LOA	ICC (95% CI)	Bias ± S.D.	LOA
Sella turcica (S)	0.983	0.0 ± 1.3	-2.5 to 2.5	0.997	0.0 ± 1.0	-2.1 to 2.1	0.999	0.0 ± 0.6	-1.3 to 1.3
Nasion (N)	0.994	-0.2 ± 0.8	-1.7 to 1.3	0.998	0.0 ± 1.0	-1.9 to 1.9	0.997	0.2 ± 1.0	-1.8 to 2.2
Point A (A)	0.995	-0.2 ± 0.7	-1.5 to 1.1	0.997	-0.1 ± 1.0	-2.1 to 1.9	0.997	-0.1 ± 0.8	-1.8 to 1.6
Point B (B)	0.991	0.0 ± 0.9	-1.7 to 1.7	0.996	-0.1 ± 1.1	-2.2 to 2.0	0.986	-0.3 ± 1.6	-3.5 to 2.9
Anterior nasal spine (ANS)	0.994	-0.4 ± 0.7	-1.8 to 1.1	0.996	-0.2 ± 1.3	-2.7 to 2.3	0.997	0.1 ± 0.9	-1.6 to 1.8
Posterior nasal spine (PNS)	0.987	-0.1 ± 1.1	-2.2 to 2.0	0.994	0.1 ± 1.5	-2.8 to 3.1	0.996	-0.2 ± 0.9	-2.1 to 1.6
Right orbital (RtOr)	0.983	-0.1 ± 1.5	-3.0 to 2.8	0.998	-0.1 ± 0.8	-1.7 to 1.5	0.998	0.0 ± 0.7	-1.4 to 1.3
Left orbital (LtOr)	0.990	0.2 ± 1.2	-2.1 to 2.6	0.995	-0.1 ± 1.3	-2.7 to 2.5	0.998	-0.2 ± 0.7	-1.5 to 1.1
Right porion (RtPo)	0.978	0.7 ± 1.7	-2.6 to 4.0	0.997	-0.4 ± 1.1	-2.5 to 1.7	0.998	0.1 ± 0.8	-1.4 to 1.6
Left porion (LtPo)	0.982	-0.4 ± 1.6	-3.5 to 2.6	0.992	-0.4 ± 1.7	-3.8 to 3.0	0.999	-0.1 ± 0.6	-1.3 to 1.2
Incisal edge of upper right central incisor (RtUI)	0.997	-0.1 ± 0.5	-1.0 to 0.9	0.996	-0.1 ± 1.1	-2.3 to 2.0	0.999	0.1 ± 0.5	-1.0 to 1.1
Incisal edge of upper left central incisor (LtUI)	0.995	0.1 ± 0.7	-1.2 to 1.4	0.997	-0.1 to 1.0	-2.2 to 1.9	0.998	0.0 ± 0.6	-1.2 to 1.3

	R			A			S		
Apical root of upper right central incisor (RtUA)	0.995	-0.2 ± 0.7	-1.5 to 1.1	0.996	-0.7 ± 1.2	-3.0 to 1.6	0.994	0.4 ± 1.0	-1.6 to 2.4
Apical root of upper left central incisor (LtUA)	0.997	-0.2 ± 0.5	-1.2 to 0.8	0.996	-0.6 ± 1.2	-3.0 to 1.8	0.993	0.4 ± 1.2	-1.9 to 2.7
Incisal edge of lower right central incisor (RtLI)	0.996	-0.1 ± 0.6	-1.3 to 1.1	0.996	-0.1 ± 1.1	-2.3 to 2.0	0.997	0.0 ± 0.7	-1.4 to 1.4
Incisal edge of lower left central incisor (LtLI)	0.997	0.1 ± 0.5	-0.9 to 1.2	0.996	-0.1 ± 1.1	-2.1 to 2.0	0.998	0.1 ± 0.6	-1.1 to 1.3
Apical root of lower right central incisor (RtLA)	0.995	0.0 ± 0.7	-1.3 to 1.2	0.996	-0.1 ± 1.1	-2.2 to 2.0	0.993	0.1 ± 1.1	-2.2 to 2.3
Apical root of lower left central incisor (LtLA)	0.997	0.0 ± 0.6	-1.1 to 1.1	0.996	0.0 ± 1.1	-2.2 to 2.3	0.995	0.2 ± 1.0	-1.8 to 2.2
Gnathion (Gn)	0.991	-0.2 ± 0.9	-1.9 to 1.5	0.995	0.0 ± 1.3	-2.5 to 2.5	0.992	0.1 ± 1.0	-1.9 to 2.1
Right gonion (RtGo)	0.999	0.2 ± 1.1	-1.8 to 2.3	0.999	-0.9 ± 1.5	-3.8 to 1.9	0.992	0.9 ± 1.5	-2.0 to 3.9
Left gonion (LtGo)	0.989	0.1 ± 1.2	-2.2 to 2.4	0.991	-0.7 ± 1.7	-4.0 to 2.6	0.994	0.4 ± 1.3	-2.1 to 2.9

Table 3
Comparison of means and standard deviations (mm) of landmark coordinates between male and female subjects

Landmarks	Mean ± S.D. (mm)								
	Males (n = 18)			Females (n = 21)			p-value		
	X	Y	Z	X	Y	Z	X	Y	Z
Sella turcica (S)	0.0 ± 0.0	0.0 ± 0.0	0.0 ± 0.0	0.0 ± 0.0	0.0 ± 0.0	0.0 ± 0.0			
Nasion (N)	1.0 ± 0.9	66.8 ± 2.3	7.6 ± 6.1	0.6 ± 1.1	63.6 ± 2.8	8.2 ± 3.0	0.327	0.000*	0.698
Point A (A)	0.7 ± 0.9	68.3 ± 3.9	-52.7 ± 6.0	0.2 ± 1.4	66.3 ± 3.0	-48.2 ± 2.8	0.181	0.072	0.004*
Point B (B)	0.1 ± 2.0	66.2 ± 6.4	-94.1 ± 8.1	-0.6 ± 2.4	63.5 ± 5.1	-89.7 ± 4.6	0.323	0.157	0.038*
Anterior nasal spine (Ans)	0.7 ± 1.0	70.0 ± 3.5	-48.1 ± 5.7	0.2 ± 1.4	68.1 ± 3.1	-43.6 ± 2.5	0.265	0.083	0.002*
Posterior nasal spine (Pns)	0.3 ± 0.7	20.7 ± 3.3	-46.4 ± 4.5	0.0 ± 1.2	20.3 ± 2.8	-41.7 ± 2.7	0.352	0.686	0.000*
Right orbital (RtOr)	35.3 ± 3.1	55.9 ± 2.2	-22.4 ± 5.1	34.1 ± 2.8	54.8 ± 2.7	-19.6 ± 2.4	0.203	0.181	0.030*
Left orbital (LtOr)	-33.3 ± 3.2	57.3 ± 2.3	-21.9 ± 5.5	-31.4 ± 2.6	55.9 ± 2.9	-18.9 ± 2.5	0.053	0.130	0.034*
Right porion (RtPo)	61.1 ± 3.4	-23.7 ± 3.0	-19.5 ± 3.5	59.3 ± 2.0	-21.4 ± 2.7	-19.0 ± 2.9	0.039*	0.013*	0.683
Left porion (LtPo)	-61.7 ± 3.5	-22.4 ± 2.7	-18.5 ± 4.1	-58.8 ± 2.5	-20.9 ± 2.7	-17.0 ± 3.0	0.005*	0.092	0.203
Incisal edge of upper right central incisor (RtUI)	5.2 ± 1.5	74.1 ± 5.6	-75.4 ± 6.5	4.1 ± 2.0	72.6 ± 3.9	-70.7 ± 3.6	0.068	0.333	0.007*
Incisal edge of upper left central incisor (LtUI)	-4.0 ± 1.3	74.2 ± 5.6	-75.5 ± 6.5	-4.6 ± 2.0	72.6 ± 3.9	-70.7 ± 3.7	0.291	0.321	0.007*
Apical root of upper right central incisor (RtUA)	4.6 ± 1.2	65.3 ± 4.2	-56.1 ± 6.1	3.7 ± 1.7	63.6 ± 3.3	-51.1 ± 3.6	0.087	0.152	0.003*

*Statistically significant differences between male and female subjects (p-value < 0.05)

Landmarks	Mean ± S.D. (mm)								
	Males (n = 18)			Females (n = 21)			p-value		
	X	Y	Z	X	Y	Z	X	Y	Z
Apical root of upper left central incisor (LtUA)	-3.5 ± 1.3	65.7 ± 4.0	-55.8 ± 6.2	-3.9 ± 1.5	63.6 ± 3.3	-51.0 ± 3.5	0.412	0.088	0.004*
Incisal edge of lower right central incisor (RtLI)	3.1 ± 2.1	71.6 ± 5.5	-73.5 ± 6.2	2.6 ± 2.0	69.7 ± 3.7	-68.5 ± 3.9	0.438	0.190	0.004*
Incisal edge of lower left central incisor (LtLI)	-2.7 ± 2.0	71.7 ± 5.4	-73.3 ± 6.2	-3.3 ± 1.9	69.7 ± 3.8	-68.4 ± 3.9	0.285	0.184	0.004*
Apical root of lower right central incisor (RtLA)	2.7 ± 2.3	64.2 ± 5.5	-89.6 ± 5.6	2.0 ± 2.4	61.6 ± 4.6	-84.6 ± 3.7	0.322	0.120	0.002*
Apical root of lower left central incisor (LtLA)	-2.5 ± 2.3	64.3 ± 5.5	-89.7 ± 5.6	-3.0 ± 2.3	61.6 ± 4.6	-84.8 ± 3.8	0.515	0.106	0.002*
Gnathion (Gn)	-0.4 ± 2.0	64.3 ± 7.4	-111.0 ± 6.8	-1.0 ± 2.7	61.3 ± 5.6	-104.7 ± 5.4	0.440	0.160	0.003*
Right gonion (RtGo)	48.3 ± 3.3	-6.4 ± 5.5	-86.3 ± 6.9	43.3 ± 3.0	-4.5 ± 3.5	-78.5 ± 4.7	0.000*	0.183	0.000*
Left gonion (LtGo)	-48.4 ± 3.1	-6.5 ± 5.8	-85.3 ± 6.6	-44.6 ± 3.2	-5.3 ± 3.8	-77.4 ± 4.8	0.001*	0.423	0.000*
*Statistically significant differences between male and female subjects (p-value < 0.05)									

Statistical analyses

All variables and measurements were imported into a Microsoft Excel spreadsheet (Version 16.0, Microsoft Corp, Redmond, WA) and then analyzed using the Statistical Package for Social Sciences (SPSS for Windows, Version 18.0, IBM Corp, Somers, NY). The intraclass correlation coefficient (ICC) obtained by comparing the values of R, A, and S, which indicate the exact location of each point on the axial, coronal and sagittal axes of the skull respectively, was calculated to assess the reliability of the measurements. The results showed an ICC range of 0.97–0.99 with a confidence interval of 0.95 (Table 2).

Bland-Altman plots were used to determine inter- and intra-examiner agreement between two measurements (Bland and Altman, 1986). They were constructed by plotting the average value of the measurements taken at two separate time points against the value difference (Figs. 2 and 3). The level of agreement (LoA) was determined as the 95% confidence intervals of the mean differences in coordinate measurements. If the LoA range contained zero, no systematic bias was determined to exist. Intra-examiner reliability of R, A, and S coordinates for each landmark is shown in Table 2.

The data were transformed in order to establish sella turcica (S) as the center point (X, Y, Z = 0, 0, 0). The normality of the landmark coordinates was determined using histograms and the Shapiro-Wilk test, and the equality of variances across data sets was determined using Levene's test. As the absolute values of the landmark coordinates were distributed normally, independent T-tests were used for gender comparison. *P* values less than 0.05 were considered statistically significant (Table 3).

Generating the 3D cephalometric template

Two 3D cephalometric template prototypes were created for Thai male and female adults utilizing the arithmetic mean of 21 landmark coordinates using 3D Builder software (Microsoft Corp, Redmond, WA). Lines were drawn connecting each coordinate to its neighboring landmark points.

Results

As seen in the 3D scatter plot (Fig. 4), male and female mean landmark coordinates are indicated by green and red dots, respectively. Cephalometric measurements between gender were significantly different, particularly in the Z direction. As a result, two distinct templates were created. A prototype of the 3D cephalometric template is shown in Fig. 5, which was then superimposed on a 3D image of the skull in Fig. 6. Figures 7 and 8 show the QR codes that lead to trial download of these templates.

Discussion

A change of dental specialty virtual treatment planning collaboration via an accurate, reproducible, and safe 3D image through digital analytics, meanwhile, requires innovation, particularly given the speed at which CBCT technology has undergone rapid evolution, and disruption are taking place. In orthodontics, 3D imaging improves diagnosis and treatment planning in a wide variety of cases, especially in orthognathic surgery and dentofacial deformities with substantial evidence for accuracy [17–20].

Nevertheless, landmark identification in 3D images is not an easy task. This may lead to inter-and intra-examiner errors. However, when associated images from multiplanar views were utilized in conjunction with 3D models, the precision of landmark localization improved[21–22]. The exact location of the mid-sella point also can be more accurately and readily identified on the 3D image due to allowance of the simultaneous visualization of all three planes[19]. Additionally, other landmarks in the midsagittal plane were more easily identified due to similarities with the 2D lateral cephalogram[23]. The landmark gnathion (Gn), on the other hand, still showed low intra-examiner correlation with respect to the Z-axis (sagittal

plane). According to Baumrind and Frantz[24], one probable explanation is that reference points located on a prominence or curvature present higher variability compared with the landmarks at defined and plane positions[25]. However, the scatter plots still revealed a normal distribution of all cephalometric landmarks made on the 3D images, as the points did not deviate too greatly from one subject to another. More importantly, our inter-examiner and intra-examiner reliability levels came within acceptable limits.

The study by Bholsithi et al.[26] focused on Thai subjects' linear and angular measurement norms in 2D and 3D cephalometric analysis, but a 3D template for the Thai population was yet to be established. Hence, from the mean coordinates of 21 commonly used cephalometric landmarks with gender dimorphism ($p < 0.05$), we have proposed two cephalometric templates for both Thai male and female adults.

To use these templates, a 3D reconstruction of the patient's skull needs to be created and converted from a .dcm to a .stl file. Several free open source software that have this capability are available, and of them, 3D Slicer is recommended. 3D Slicer is compatible with any computer operating on Windows, Mac, or Linux systems released within the last five years, although older systems may be able to operate the software depending mainly on the graphics capabilities. The CBCT data in .dcm format can be processed in the 'Segment Editor' module to produce a reconstructed 3D model of the skull that can be exported as a .stl file.

Strengths

The strength of this study is that it creates a cutting-edge cephalometric norm in the form of virtual reality from the freeware available. Therefore, this method can be practically and economically repeated to create cephalometric norms for any racial group. This innovation also paves way to the futuristic orthodontic consultation. The 3D cephalometric template can be superimposed on the 3D model of the skull using the freeware 3D Builder. This software would enable any clinicians to examine the dysmorphology of facial structures without requiring to plot landmarks beforehand.

Moreover, there are numerous technological devices available today that can be utilized for viewing 3D models, including mixed reality (MR) headsets, Xbox consoles, personal computers, smartphones, or tablets. With the aid of technological advancements, various medical specialties would be able to codevelop better and easier diagnoses and treatment plans.

In detail, MR is the merging of the real and virtual worlds to produce new environments and visualizations, where physical and digital objects co-exist and interact in real time. MR does not exclusively take place in either the physical world or virtual world, but is a hybrid of augmented reality and virtual reality. An exciting application would be the incorporation of MR headsets like the Microsoft HoloLens and smart-glasses into patient examination to aid in orthodontic diagnosis and treatment planning. For instance, the 3D cephalometric template of the population norm could be conveniently displayed together with the patient's 3D skull CBCT model, while overlaying precise visual guides for the clinicians. MR may open up a vast array of possibilities for enhancing the explanation of the virtual plan

not only for patients but also for virtual planning among different medical and dental specialties. Additionally, at this stage of pandemic, MR combining these cephalometric templates with patients' reality enhances the teledentistry consultation. This user-friendly virtual media can also be used with metaverse. It can be used in a virtual meeting by many dental specialties, patient(s) with guardians, partners, or relatives in the very near future.

Limitations

At the time of writing, there are currently no other 3D cephalometric templates available for the Asian population. The templates developed from our study are most effective when applied to Thai adults, therefore caution should be taken if these templates are applied to patients in other regions, although Cambodian and Vietnamese skull measurements were found to be highly similar to those of Thais[27–29].

As the sample size in this study was rather limited, additional research with a more extensive sample size should be conducted to better represent the diversity in the population. Another required aspect would be the development of an easily accessible and user-friendly computer platform for the use of this 3D craniofacial analysis.

Moreover, the future development of 3D cephalometric templates may serve as a bridge for future studies and analyses that move beyond linear and angular measurements, especially when all these limitations are considered. Finally, the rapid growth in imaging technology should be taken advantage of by reconsidering advanced methods of skeletal analysis, specifically with the use of AI and machine learning [30].

Conclusion

Thai adult male and female 3D cephalometric templates have been developed to provide an easily comprehensible assessment of deviations in craniofacial structures from the norm. These templates can be superimposed on the 3D-reconstructed image of the skull obtained from the CBCT .dcm file. These 3D cephalometric templates have the potential to pave the way towards AI-assisted orthodontic diagnosis and treatment planning.

Abbreviations

2D: Two-dimensional;

3D: Three-dimensional;

AI: Artificial intelligence;

ML: Machine learning

Declarations

Acknowledgements

Not applicable.

Authors' contributions

J.D., S.M., S.T., contributed to conception, design, analysis, and interpretation, drafted and critically revised the manuscript; S.R., contributed to conception, data acquisition and interpretation, drafted and critically revised the manuscript. J.D. prepared all figures and tables. All authors gave the final approval and agreed to be accountable for all aspects of the work.

Funding

Funding was obtained from Mahidol university.

Availability of data and materials

The datasets used and/or analyzed in the current study are available from the corresponding author on reasonable request. (Somchai Manopatanakul, msomchai@rocketmail.com)

Ethics approval and consent to participate

The ethical approval of this study was obtained from the Institutional Review Board of the Faculty of Dentistry/Faculty of Pharmacy, Mahidol University (COE. No. MU-DT/PY-IRB 2020/084.2412). Before conducting the research, written informed consents were also obtained from all participants and parents/guardians of the participants. All methods were carried out in accordance with International guideline for human research protection (Declaration of Helsinki).

Consent for publication

Not applicable.

Competing interests

The authors declare that they have no competing interests.

References

1. Lemieux G, Carey JP, Flores-Mir C, Secanell M, Hart A, Dietrich N, et al. Three-dimensional cephalometric superimposition of the nasomaxillary complex. Am J Orthod Dentofacial Orthop. 2014;146(6),758-64. http://dx.doi.org/10.1016/j.ajodo.2014.08.014
2. Porto OCL, de Freitas JC, de Alencar AHG, Estrela C. The use of three-dimensional cephalometric references in dentoskeletal symmetry diagnosis. Dental Press J Orthod. 2014;19(6),79-85. http://dx.doi.org/ 10.1590/2176-9451.19.6.078-085.oar

3. Alamri HM, Sadrameli M, Alshalhoob MA, Sadrameli M, Alshehri MA. Applications of CBCT in dental practice: A review of the literature. Gen Dent. 2012;60(5):390-400.
4. Kapila SD, Nervina JM. CBCT in orthodontics: Assessment of treatment outcomes and indications for its use. Dentomaxillofac Radiol. 2015;44(1):20140282. http://dx.doi.org/10.1259/dmfr.20140282
5. Mah JK, Huang JC, Choo HR. Practical applications of cone-beam computed tomography in orthodontics. J Am Dent Assoc. 2010;14(Suppl 3),7s-13s. http://dx.doi.org/ 10.14219/jada.archive.2010.0361
6. da Silva MBG, Sant'Anna EF. The evolution of cephalometric diagnosis in Orthodontics. Dental Press J Orthod. 2013;18(3),63-71. http://dx.doi.org/10.1590/S2176-94512013000300011
7. Kaur A, Singh C. Automatic cephalometric landmark detection using Zernike moments and template matching. SIViP. 2015;9(1),117-32. http://dx.doi.org/ 10.1007/s11760-013-0432-7
8. Park SH, Yu HS, Kim KD, Lee KJ, Baik HS. A proposal for a new analysis of craniofacial morphology by 3-dimensional computed tomography. Am J Orthod Dentofacial Orthop. 2006;129(5),600.E23-600.E34. http://dx.doi.org/ 10.1016/j.ajodo.2005.11.032
9. Naji P, Alsufyani NA, Lagravère MO. Reliability of anatomic structures as landmarks in three-dimensional cephalometric analysis using CBCT. Angle Orthod. 2014;84(5),762-72. http://dx.doi.org/ 10.2319/090413-652.1
10. Chalipa J, Akhoundi MSA, Shoshtarimoghaddam E, Nik TH, Imani M. Designing orthodontic craniofacial templates for 8-14 year-old Iranian girls based on cephalometric norms. J Dent (Tehran). 2013;10(1),64-73.
11. Jacobson A. The proportionate template as a diagnostic aid. Am J Orthod. 1979;75(2),156-72. http://dx.doi.org/10.1016/0002-9416(79)90185-4
12. Moorrees CFA, van Venrooij ME, Lebret LML, Glatky CB, Kent RL, Reed RB. New norms for the mesh diagram analysis. Am J Orthod. 1976;69(1),57-71. http://dx.doi.org/10.1016/0002-9416(76)90098-1
13. Harris JE, Johnston L, Moyers RE. A cephalometric template: Its construction and clinical significance. Am J Orthod. 1963;49(4):249–63. http://dx.doi.org/10.1016/0002-9416(63)90002-2
14. Liebgott B. Cephalometric analysis using a template. Angle Orthod. 1978;48(3):194–201.
15. Fedorov A, Beichel R, Kalpathy-Cramer J, Finet J, Fillion-Robin JC, Pujol S, et al. 3D Slicer as an image computing platform for the quantitative imaging network. Magn Reson Imaging. 2012;30(9),1323-41. http://dx.doi.org/10.1016/j.mri.2012.05.001
16. Zamora N, Llamas JM, Cibrián R, Gandia JL, Paredes V. Cephalometric measurements from 3D reconstructed images compared with conventional 2D images. Angle Orthod. 2011;81(5),856-64. http://dx.doi.org/10.2319/121210-717.1
17. Lee M, Kanavakis G, Miner RM. Newly defined landmarks for a three-dimensionally based cephalometric analysis: A retrospective cone-beam computed tomography scan review. Angle Orthod. 2015;85(1),3-10. http://dx.doi.org/10.2319/021814-120.1

18. de Oliveira AEF, Cevidanes LHS, Phillips C, Motta A, Burke B, Tyndall D. Observer reliability of three-dimensional cephalometric landmark identification on cone-beam computerized tomography. Oral Surg Oral Med Oral Pathol Oral Radiol Endod. 2009;107(2),256-65. http://dx.doi.org/10.1016/j.tripleo.2008.05.039
19. Periago DR, Scarfe WC, Moshiri M, Scheetz JP, Silveira AM, Farman AG. Linear accuracy and reliability of cone beam CT derived 3-dimensional images constructed using an orthodontic volumetric rendering program. Angle Orthod. 2008;78(3),387-95. http://dx.doi.org/10.2319/122106-52.1
20. Yitschaky O, Redlich M, Abed Y, Faerman M, Casap N, Hiller N. Comparison of common hard tissue cephalometric measurements between computed tomography 3D reconstruction and conventional 2D cephalometric images. Angle Orthod. 2011;81(1),11-16. http://dx.doi.org/10.2319/031710-157.1
21. Hassan B, Nijkamp P, Verheij H, Tairie J, Vink C, van der Stelt P, et al. Precision of identifying cephalometric landmarks with cone beam computed tomography in vivo. Eur J Orthod. 2013;35(1),38-44. http://dx.doi.org/10.1093/ejo/cjr050
22. da Neiva MB, Soares ÁC, de Oliveira Lisboa C, de Vasconcellos Vilella O, Motta AT. Evaluation of cephalometric landmark identification on CBCT multiplanar and 3D reconstructions. Angle Orthod. 2015;85(1),11-17. http://dx.doi.org/10.2319/120413-891.1
23. Schlicher W, Nielsen I, Huang JC, Maki K, Hatcher DC, Miller AJ. Consistency and precision of landmark identification in three-dimensional cone beam computed tomography scans. Eur J Orthod. 2012;34(3),263-75. http://dx.doi.org/10.1093/ejo/cjq144
24. Baumrind S, Frantz RC. The reliability of head film measurements. 1. Landmark identification. Am J Orthod. 1971;60(2),111-27. http://dx.doi.org/10.1016/0002-9416(71)90028-5
25. Sam A, Currie K, Oh H, Flores-Mir C, Lagravére M, Lagravére-Vich L. Reliability of different three-dimensional cephalometric landmarks in cone-beam computed tomography: A systematic review. Angle Orthod. 2019;89(2):317-32. http://dx.doi.org/10.2319/042018-302.1
26. Bholsithi W, Tharanon W, Komolpis R, Sinthanayothin C. 3D vs. 2D cephalometric analysis comparisons with repeated measurements from 20 Thai males and 20 Thai females. Biomed Imaging Interv J. 2009;5(4):e21. http://dx.doi.org/10.2349/biij.5.4.e21
27. Pietrusewsky M. A multivariate analysis of measurements recorded in early and more modern crania from East Asia and Southeast Asia. Quat Int. 2010;211(1–2):42–54. http://dx.doi.org/10.1016/j.quaint.2008.12.011
28. Kiim J, Gansukh O, Amarsaikhan B, Lee S, Kim T. Comparison of cephalometric norms between Mongolian and Korean adults with normal occlusions and well-balanced profiles. Korean J Orthod. 2011;41(1):42–50. http://dx.doi.org/10.4041/kjod.2011.41.1.42
29. Cooke M, Wei SHY. A comparative study of southern Chinese and British Caucasian cephalometric standards. Angle Orthod. 1989;59(2):131–8.
30. Lee JH, Yu HJ, Kim MJ, Kim JW, Choi J. Automated cephalometric landmark detection with confidence regions using Bayesian convolutional neural networks. BMC Oral Health. 2020;20(1):270.

https://doi.org/10.1186/s12903-020-01256-7

Figures

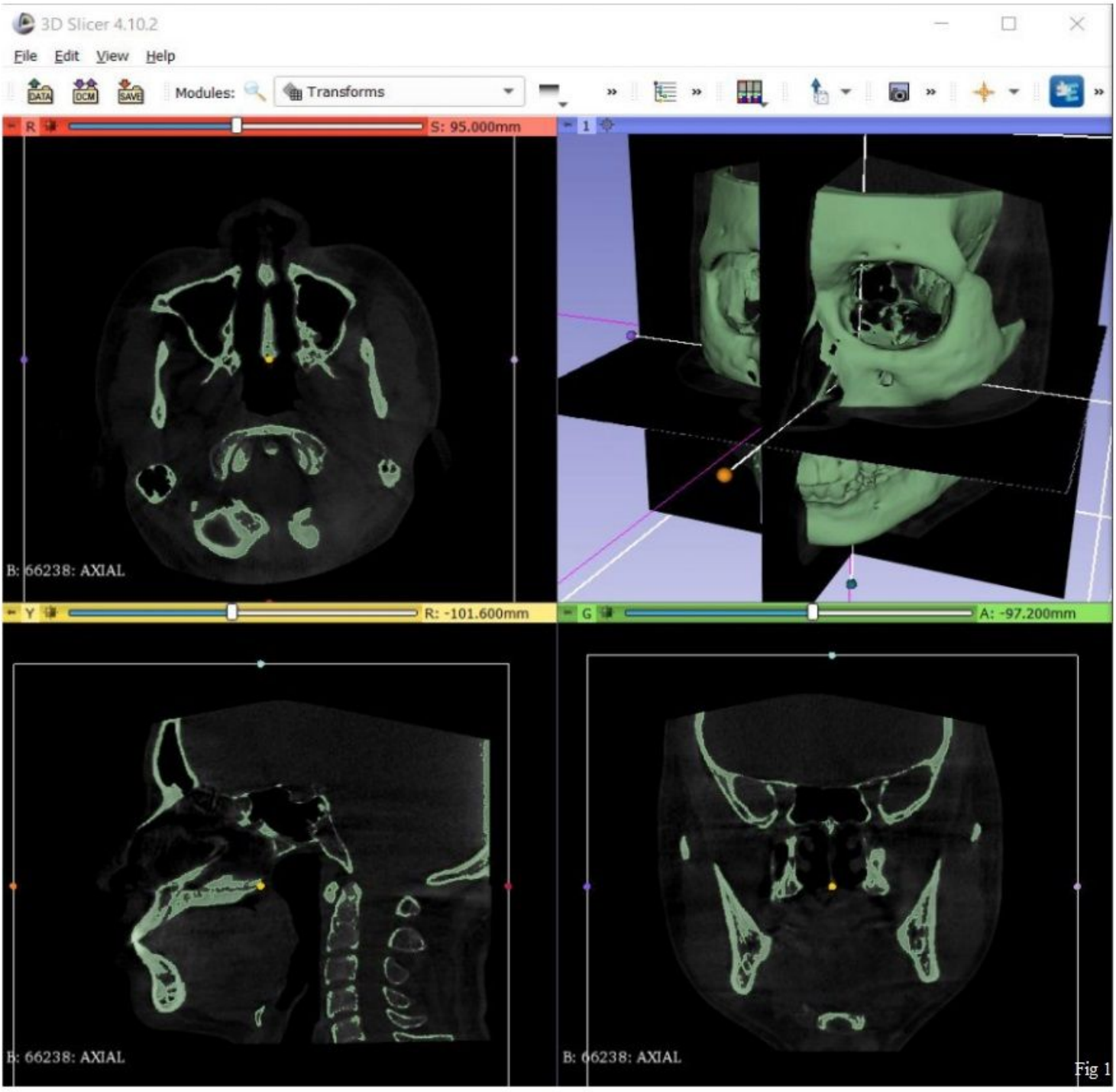

Figure 1

Anatomical landmark identification using Slicer 4.10.2 software enables simultaneous viewing of the same spatial point in the sagittal, coronal, and axial planes, as well as on a 3D image in four separate windows.

This figure was drawn on 3D Slicer software (version 4.10.2) which is a freeware.

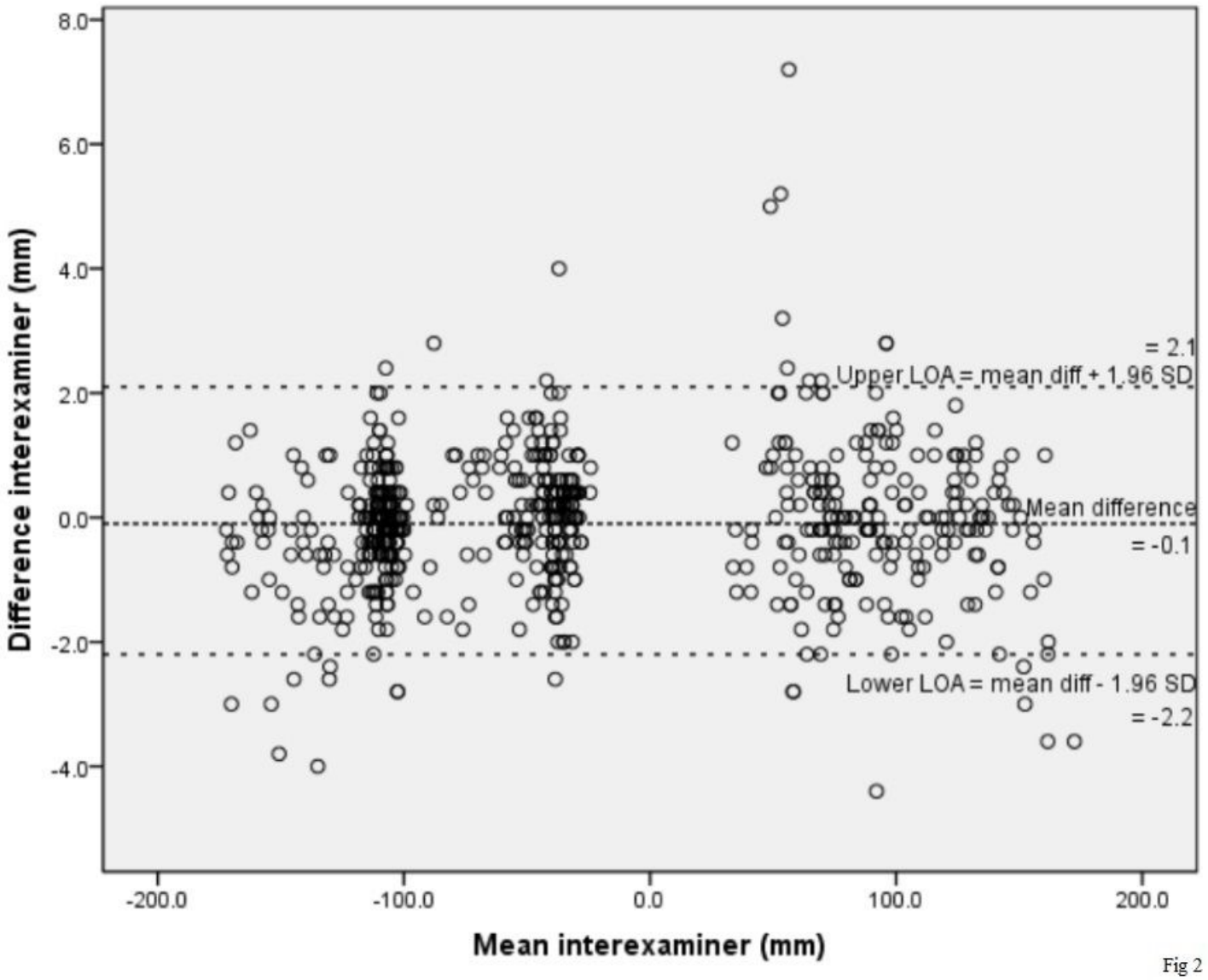

Figure 2

Bland-Altman plot for the means of coordinates measured by both the orthodontic specialist and the practitioner against the differences between measurements by the orthodontic specialist and practitioner; LOA = limits of agreement.

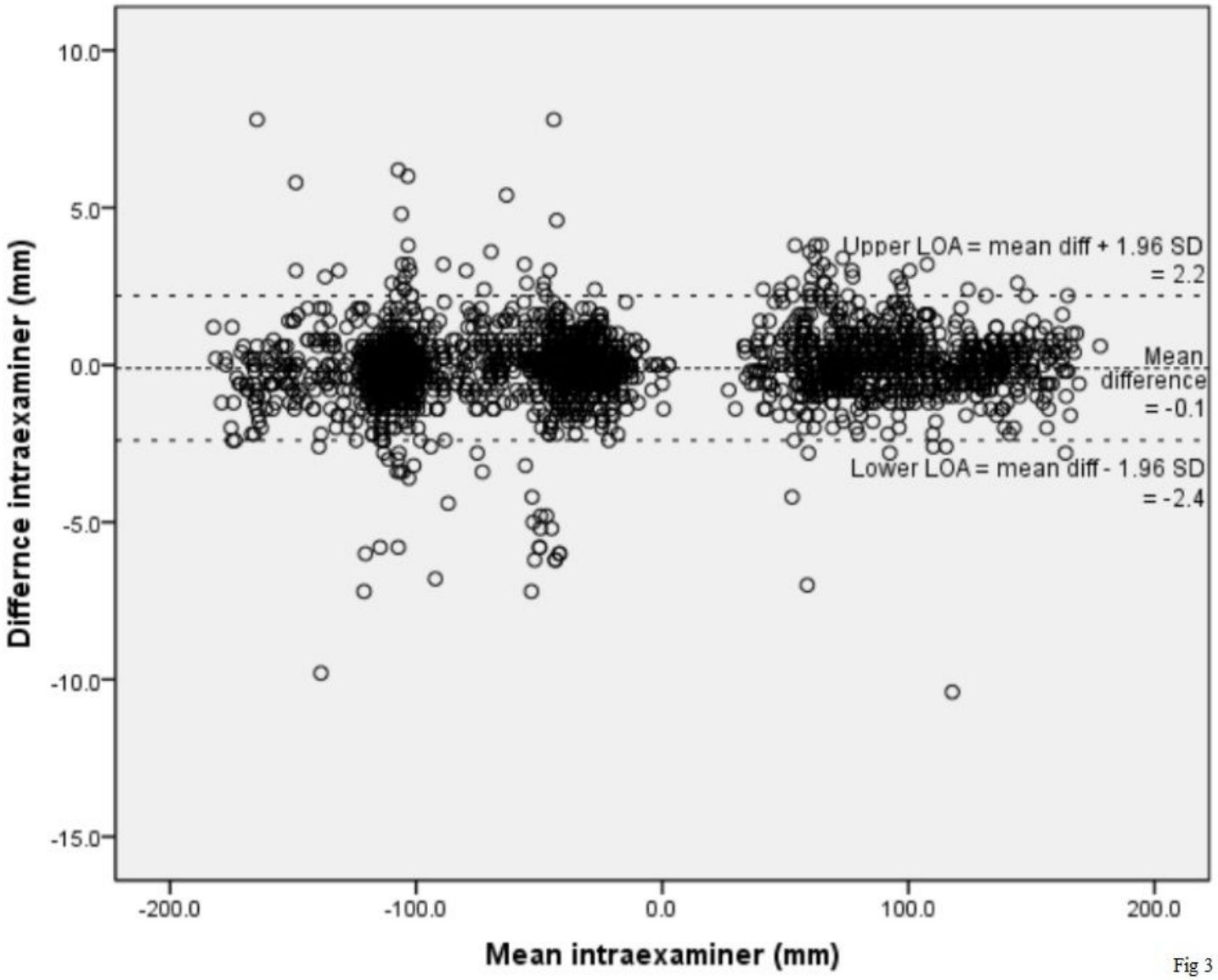

Figure 3

Bland-Altman plot for the means of coordinates of the first and second measurements by the practitioner against the difference between the first and second measurements by the practitioner; LOA = limits of agreement.

These two figures were drawn and retrieved from licensed software (SPSS) bought by Mahidol University.

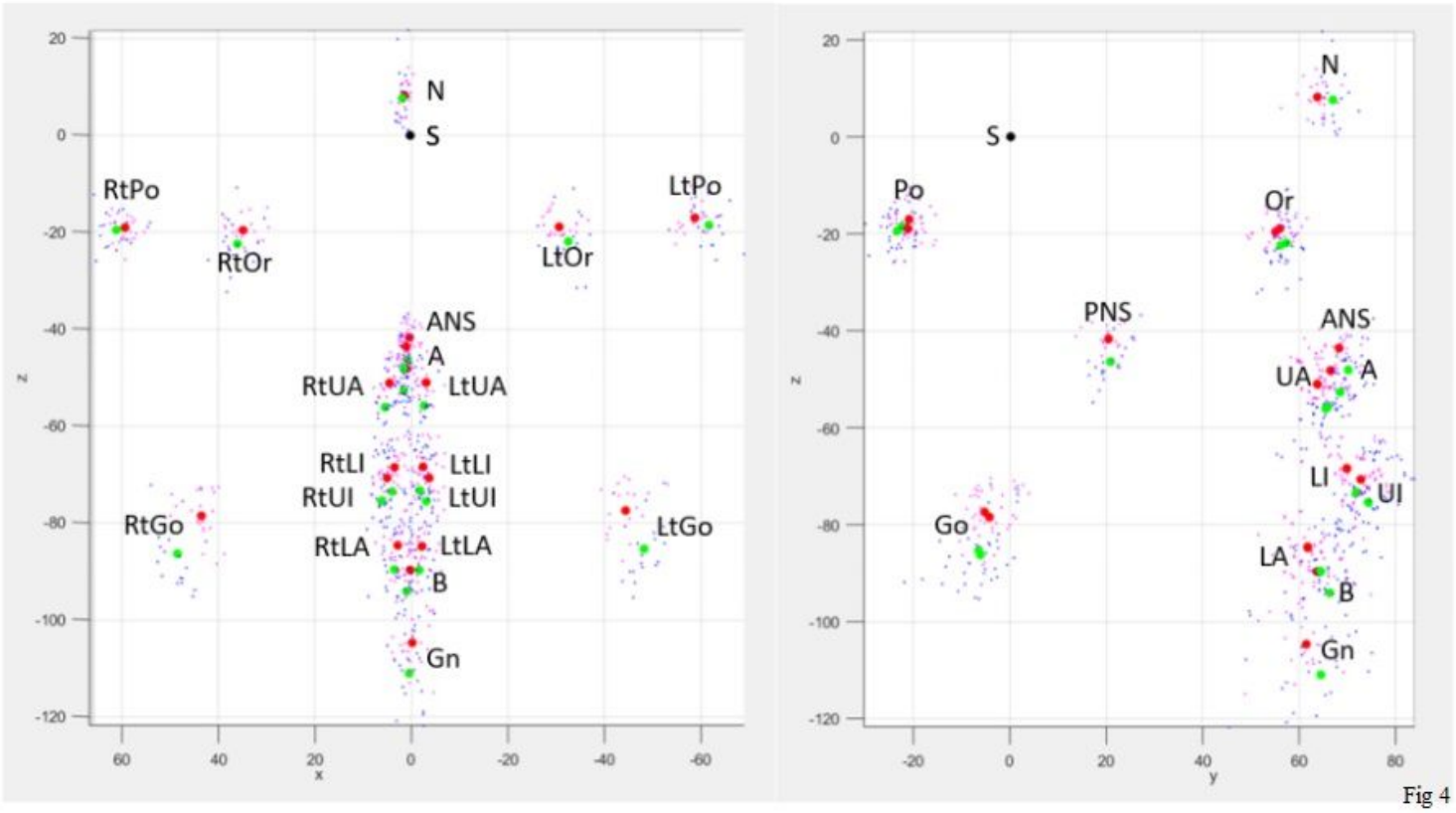

Figure 4

A 3D scatterplot to visualize the average landmark coordinates. (Green points: Male subjects; Red points: Female subjects)

This figure was drawn and retrieved from licensed software (Matlab) bought by Mahidol University.

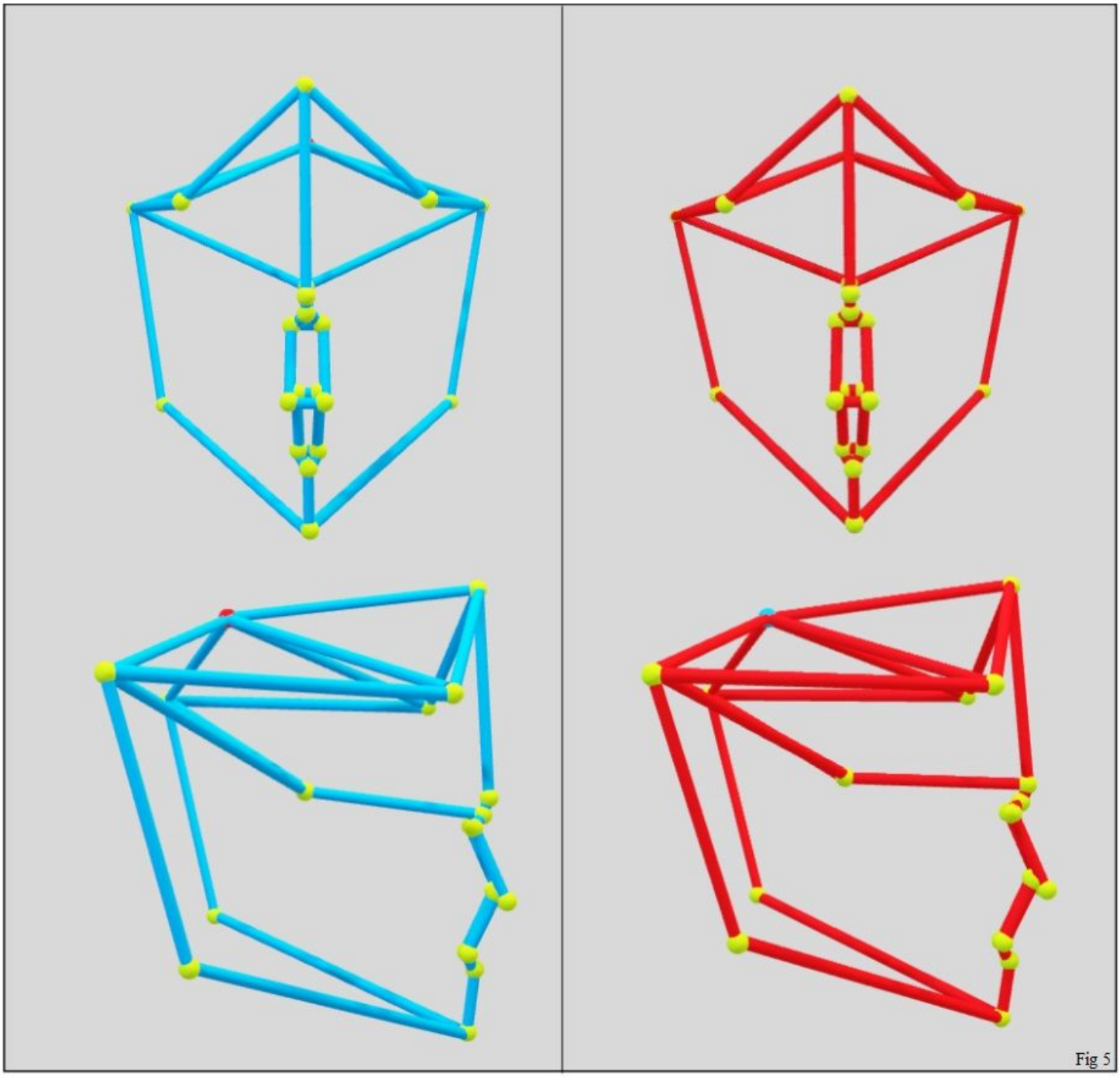

Figure 5

The 3D cephalometric template prototype, for adult Thai males (left) and females (right).

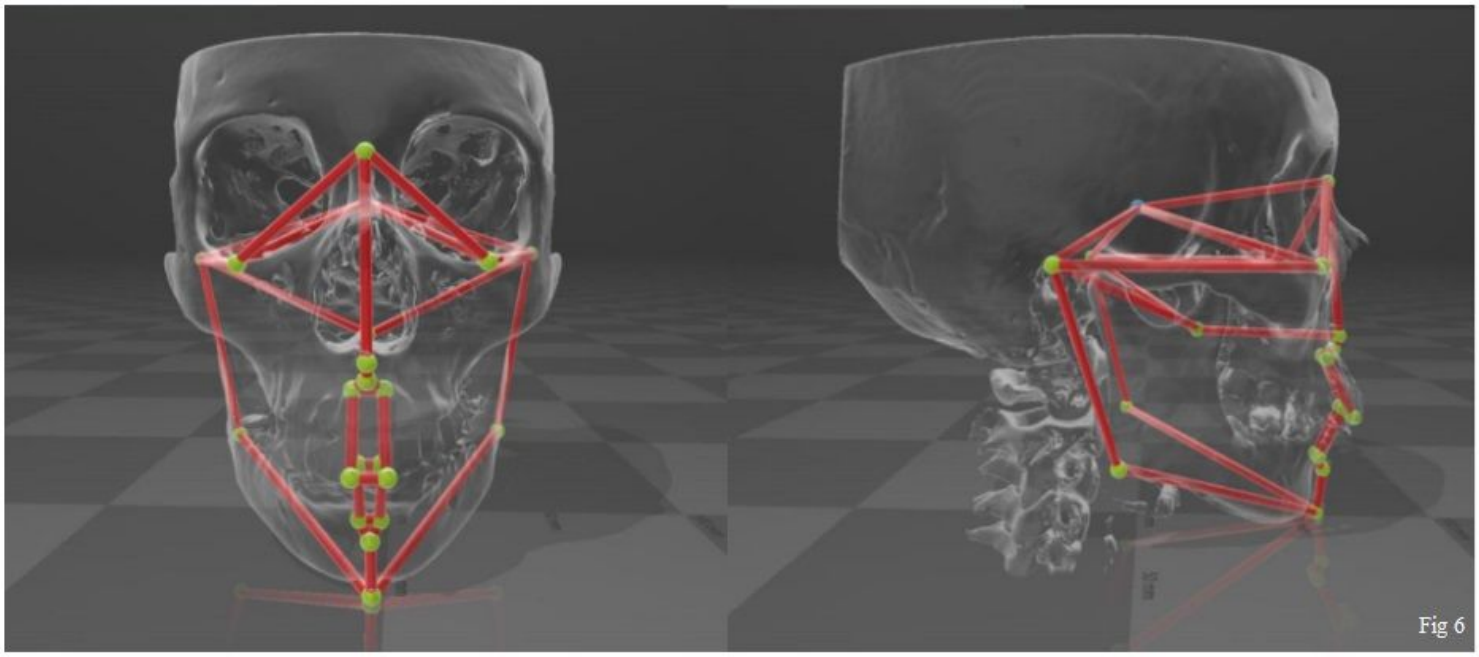

Figure 6

Superimposition of the 3D cephalometric male template onto a representative 3D skull image.

These two figures were drawn on 3D Builder software (Microsoft Corp, Redmond, WA) which at the stage of drawing is a freeware.

Figure 7

QR code for downloading the 3D cephalometric template for adult Thai males.

Figure 8

QR code for downloading the 3D cephalometric template for adult Thai females.

These two QR codes were created and retrieved from website http://th.qr-code-generator.com/ which provides free QR code production service.